

Analysis and Modeling of Electro Discharge Machining Input Parameters of Nitinol Shape Memory Alloy by De-ionized Water and Copper Tools

Esmail Abedi^{1,*}, Saeed Daneshmand¹, Ali Akbar Lotfi Neyestanak², Vahid Monfared³

¹Department of Mechanical Engineering, Majlesi Branch, Islamic Azad University, Isfahan, Iran

²Department of Mechanical Engineering, Shahre Rey Branch, Islamic Azad University, Tehran, Iran

³Department of Mechanical Engineering, Zanzan Branch, Islamic Azad University, Zanzan, Iran

*E-mail: s.daneshmand@iaumajlesi.ac.ir

Received: 31 December 2013 / Accepted: 7 February 2014 / Published: 23 March 2014

Nowadays, NiTi alloy is one of the shape memory alloys that its applications have grown in all industries. Its unique properties compared with some mechanical and thermo dynamical parameters lead in being applicable in industries such as aerospace, medicine and automobile. In the present study, EDM was modeled on NiTi alloy by means of de-ionized water and copper tools. EDM technique has different input parameters which influence on the outputs. Machining duration and process instability increase by experimental setting of input parameters. A mathematical modeling is required to make a precise relation between input and output parameters. The experiments were chosen by Design of Experiments (DOE)'s technique. Material removal rate and surface roughness were modeled with machining parameters and regression equations. The results were studied by variance analysis (ANOVA) and the most precise model was chosen as final model. Suggested model helps to find the parameters which have the most effects on material removal rate and surface roughness of NiTi alloy using de-ionized water and copper tools. Thus, material removal rate and surface roughness can be predicted.

Keywords: Electro discharge machining; Shape memory alloys; Modeling; Material removal rate; Tool wear rate; Surface roughness; Nitinol; Cu electrode

1. INTRODUCTION

Electro Discharge Machining (EDM) is an electro thermal nontraditional machining process, where electrical energy is used to generate electrical spark and material removal mainly occurs due to thermal energy of the spark. EDM is mainly used to machine difficult-to-machine materials and high

strength temperature resistant alloys [1]. EDM can be used to machine difficult geometries in small batches or even on job-shop basis. Work material to be machined by EDM has to be electrically conductive. In EDM, a potential difference is applied between the tool and workpiece. Both the tool and the work material are to be conductors of electricity [2]. The tool and the work material are immersed in a dielectric medium. Generally kerosene or deionised water is used as the dielectric medium. A gap is maintained between the tool and the workpiece. Depending upon the applied potential difference and the gap between the tool and workpiece, an electric field would be established [3]. EDM machines can be also know as vertical, ram, solid or die sinking machines. These types of machines have an electrode mounted in mainly in the Z axis. They are used to remove broken taps, spark cavities into components, produce complex internal spines and gears etc. The electrode and workpiece are connected to a suitable power supply. The power supply generates an electrical potential between the two parts. As the electrode approaches the workpiece, dielectric breakdown occurs in the fluid forming an ionization channel, and a small spark jumps [4]. The resulting heat and cavitation vaporize the base material, and to some extent, the electrode. These sparks strike one at a time in huge numbers at seemingly random locations between the electrode and the workpiece. As the base metal is eroded, and the spark gap subsequently increased, the electrode is lowered automatically by the machine so that the process can continue uninterrupted. Several hundred thousand sparks occur per second in this process, with the actual duty cycle being carefully controlled by the setup parameters.

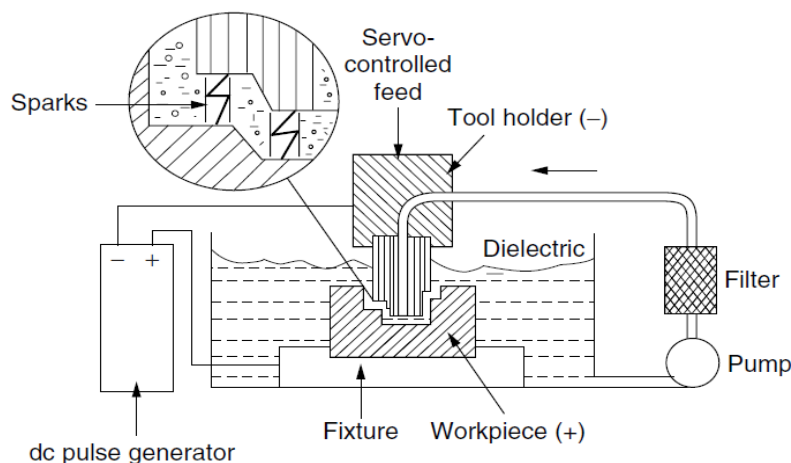


Figure 1. Schematic diagram of EDM [5]

Shape Memory Alloys (SMA's) are novel materials which have the ability to return to a predetermined shape when heated. When an SMA is cold, or below its transformation temperature, it has a very low yield strength and can be deformed quite easily into any new shape-which it will retain. However, when the material is heated above its transformation temperature it undergoes a change in crystal structure which causes it to return to its original shape [6]. If the SMA encounters any resistance during this transformation, it can generate extremely large forces. This phenomenon provides a unique mechanism for remote actuation. The most common shape memory material is an alloy of nickel and titanium called Nitinol. This particular alloy has very good electrical and mechanical properties, long fatigue life, and high corrosion resistance. The SME occurs due to a

temperature and stress dependent shift in the material's crystalline structure between two different phases, martensite (low temperature phase) and austenite (high temperature phase). The temperature, where the phase transformation occurs, is called the transformation temperature. Figure 2 is a simplified representation of material's crystalline arrangement during different phases.

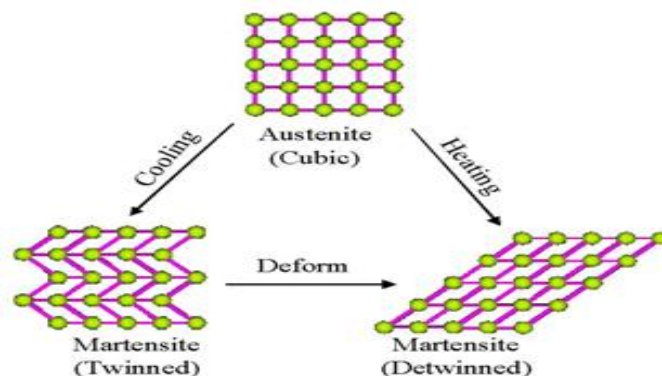


Figure 2. The Shape Memory Effect Process [7]

In austenite phase, the structure of the material is symmetrical; each grain of material is a cube with right angles. When the alloy cools, it forms the martensite phase and collapses to a structure with different shape. If an external stress is applied, the alloy will yield and deform to an alternate state. Now, if the alloy is heated again above the transformation temperature, the austenite phase will be formed and the structure of the material returns to the original cubic form, generating force/stress. The ability of SMA to recover a specific shape upon heating and then return to an alternate shape when cooled (below the transformation temperature) is known as two-way shape memory. However, there are limitations that reduce the usability of the two-way effect, such as smaller strains (2 %), extremely low cooling transformation forces and unknown long-term fatigue and stability [8]. SMA also shows a superelastic behavior if deformed at a temperature which is slightly above their transformation temperatures. This effect is caused by the stress-induced formation of some martensite above its normal temperature. Because it has been formed above its normal temperature, the martensite reverts immediately to un deformed austenite as soon as the stress is removed. The greatest advantage of the SMA material is the availability of a large force from very small element dimensions and weight. SMA alloys provide a large deformation, compared to other active materials. Maximum deformation is approximately 7...8 % for NiTi element. SMA materials offer interesting possibilities for actuator applications. The benefits such as, a large force with small dimensions and weight, a large deformation and relatively simple heating and cooling arrangements give opportunities to design micro-scale devices [9]. In spite of significant progress in traditional machining, there are many problems in machining of memory alloys, non-metal alloys and super alloys. Main objectives of machining process are cost reduction, machining speed improvement, proper dimensions and surface roughness. They are particularly are so important in machining of expensive material like NiTi alloys. The wide range of EDM's applications leads in lots of investigations in this process modeling. Kao (2001) used neural network MLP to classify different types of pulses and then to control EDM machine [10]. Indurkya and Rajurkar (2002) did researches on EDM process modeling by electrode rotation [11]. Zawada and

Niranjan applied MLP networks to monitor tool corrosion [12, 13]. Li and Tarnng used adaptive resonance theory based neural networks to study tool fracture [14, 15]. The present research focuses on introducing a mathematical model to make a relation between EDM's input and output parameters. An appropriate model for NiTi machining will be available by identifying and controlling the parameters that influence on surface roughness and material removal rate.

2. EQUIPMENTS AND METHODOLOGY

NiTi60 shape memory alloy was chosen for machining due to its capability and application. This alloy was cut and ground by wire cut machine in dimensions of $15 \times 15 \times 15\text{mm}^3$. A copper tool electrode of $15 \times 20\text{mm}^2$ was prepared. Spark machine model M204H manufactured by Tehran Ekram Engineering Co. was applied to do the tests. De-ionized water was utilized as the dielectric considering NiTi's intelligence. AND GR-300 laboratory balance with 0.0001 resolutions was used to measure the material removal volume and tool corrosion. Mahr M300-RD18 roughness measurement device was applied to measure the surface roughness of the work piece. The mechanical and physical properties of NiTi60 alloy and copper electrode are given in tables 1 and 2 [16, 17]. Design of experiments was used to do the tests. L9 orthogonal array with voltage repetition level of 30 and 200 was applied to design the experiment. In the present research the numbers of experiments and factors are 9 and 4, respectively.

Table 1. Mechanical and physical properties of NiTi60 [17]

Density	6.45 G/cc
Tensile strength, ultimate	754 - 960 Mpa
Tensile strength, yield	560 Mpa
Elongation at break	15.5 %
Modulus of elasticity	75.0 Gpa
Shear modulus	28.8 Gpa
Thermal conductivity	10.0 W/m-k
Melting point	1240 - 1310 °C
Nickel, Ni	60.0 %
Titanium, Ti	40.0 %

Table 2. Physical properties of copper electrode [16]

Physical properties	Copper
Thermal conductivity [W/m·K]	380.7
Melting point [°C]	1083
Boiling temperature [°C]	2595
Specific heat [cal/g·°C]	0.092
Specific gravity at 20°C [g/cm ³]	8.9
Coefficient of thermal expansion [$\times 10^{-6}$ (1/°C)]	17

Input parameters are voltage, current, pulse on time and pulse off time. Output parameters include material removal rate, tool corrosion and surface roughness. Specifications and input parameters applied in the experiment are presented in table 3. Input parameter of the experiments shown in table 4.

Table 3. Process parameters and their levels

Experiment variable	Descriptions
Generator mode	Iso pulse
Power supply voltage (V)	30, 200
Tool polarity	Positive
Dielectric fluid	De-ionized
Flashing type	Normal submerged
Discharge current (A)	10, 15, 20
Pulse on time (μs)	35, 50, 100
Pulse off time (μs)	30, 70, 200

Equations 1 and 2 were applied to calculate material removal rate and relative tool erosion [18].

$$MRR = \frac{M_{W1} - M_{W2}}{\rho_w \times t} \times 10^3 \tag{1}$$

$$TWR = \frac{(M_{T1} - M_{T2})\rho_w}{(M_{W1} - M_{W2})\rho_T} \times 100 \tag{2}$$

ρ_T and ρ_w : Density of tool and workpiece

t: Machining duration

MRR: Material removal rate

TWR: Tool wear rate

M_{w1} and M_{w2} : work piece weight before and after machining

M_{T1} and M_{T2} : tool weight before and after machining

L9 orthogonal Taguchi array leads in 9 tests was chosen considering degrees of freedom of the system. Input parameter of the experiment is shown in table 3. Material removal rate and surface roughness values are given in table 5 for 9 tests according to different control levels.

Table 4. Levels for various control factors

Control factors	Voltage	Pulse on time	Current	Pulse off time
Level 1	80	25	10	30
Level 2	250	10	15	70
Level 3	80	100	20	100

Table 5. L9 Orthogonal array

Sl. No	Voltage	Pulse on time	Discharge current	Pulse off time	Surface Roughness (Ra)	Material removal rate (MRR)
1	1	1	1	1	3.22800	0.74935
2	2	2	2	1	2.64767	1.11111
3	3	3	3	1	4.98133	3.38501
4	3	2	1	2	3.00967	1.52455
5	1	3	2	2	5.53500	4.78036
6	2	1	3	2	3.80967	2.48062
7	2	3	1	3	2.37800	2.63566
8	3	1	2	3	2.95900	0.54264
9	1	2	3	3	3.67300	2.29974

3. MATERIAL REMOVAL RATE MODELING

Regression functions, experimental data, determination of main factors and noticeable effects on material removal rate were used to model material removal rate of NiTi alloy by copper electrode and de-ionized water. Variance analysis of material removal rate for NiTi is given in table 6. The effects of spark current intensity, pulse on time and pulse off time are respectively main and critical effects of the process to achieve 95% confidence level with $P < 0.050$.

Table 6. Analysis of variance for material removal rate

Source	Degrees of freedom (DF)	Sum of squares (SS)	Mean square (MS)	F-ratio	P-value
Voltage	1	2.6	2.60	1.49	0.261
On Time	2	1.77	0.88	0.41	0.683
Current	2	9.462	4.731	5.29	0.047
Off Time	2	0.98	0.49	0.21	0.815

$$MRR = 2.56028 + 0.00628578 V + 0.0718098 T_{on} - 0.670435 I - 0.0236168 T_{of} - 3.43647E-4 T_{on}^2 + 0.0313523 I^2 + 8.32827E-5 T_{of}^2 - 5.81395E-4 T_{on} I \tag{3}$$



Figure 3. EDM machined samples

Equation 3 indicates material removal rate model for NiTi shape memory alloy with copper electrode according to input parameters of electro discharge machining. This model makes a proper relationship between input parameters of electro discharge machining and material removal rate. According to this equation, there is no need for different tests to gain material removal rate. EDM machined samples are illustrated in figure 3.

Relative error of equation 3 compared with scientific results is given in table 7. According to the results shown in this table, maximum and average errors are 17.951E-4 and %5.0006867 respectively which can be ignored because of their small amounts.

Table 7. Scrutiny regression equation calculation error (Equation 3) with experimental result

Experimental number	MRR experimental result	MRR regression equation	Error %
1	0.74935	0.749360	8.007E-4
2	1.11111	1.11112	8.342E-4
3	3.38501	3.38503	5.164E-4
4	1.52455	1.52456	7.049E-4
5	4.78036	4.78037	2.337E-4
6	2.48062	2.48063	3.658E-4
7	2.63566	2.63567	4.416E-4
8	0.54264	0.542645	17.951E-4
9	2.29974	2.29975	4.882E-4

The effects of voltage, pulse on time and pulse off time on material removal rate are illustrated in figure 4. According to equation 4, increase in pulse on time and particularly in pulse current causes increase in spark energy and higher material removal rate [18].

$$W_{av} = I_{sp} \times V_{sp} (T_{on} - T_d) \tag{4}$$

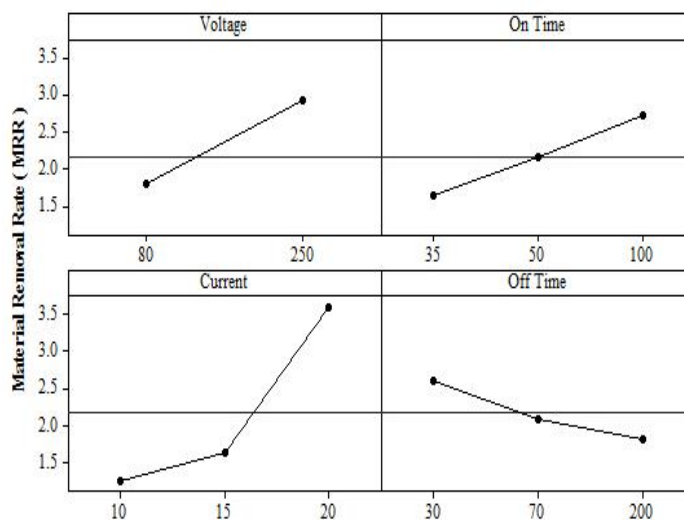


Figure 4. Effect of input parameters on MRR

4. SURFACE ROUGHNESS MODELING

Analysis of second order variance for surface roughness with 95% confidence level and $P < 0.050$ is given in table 8. Considering the results obtained from NiTi machining by copper electrode and de-ionized water pulse on time is considered the most important parameter and pulse off time, current intensity and voltage are respectively the main and critical effects of the process. Equation 5 is surface roughness model for machining NiTi60 with copper tool in which Ra, I, T_{on} and T_{off} are surface roughness, current intensity pulse on time and pulse off time respectively. Comparison between experimental results and the error caused by equation 5 is given in table 9. According to this table, the maximum and average errors of the model are %27.468E-4 and %0.0014853 respectively which are ignorable due to their small amounts. Therefore, equation 5 presents suitable results for surface roughness of shape memory alloy with copper electrode and de-ionized water. The effects of EDM's input parameters on surface roughness are illustrated in figure 5. By increasing in pulse current spark energy will be increased which leads in deeper melting hole and subsequently rise in surface roughness.

$$Ra = 8.26994 + 0.00814195 V + 0.0487479 T_{on} - 1.03422 I - 0.0223952 T_{of} - 7.27966E-04 T_{on}^2 + 0.0282022 I^2 + 7.78133E-05 T_{of}^2 + 0.00461750 T_{on} I \tag{5}$$

Table 8. Analysis of variance for surface roughness

Source of variation	Degrees of freedom (DF)	Sum of squares (SS)	Mean square (MS)	F-ratio	P-value
Voltage	1	1.30	1.30	1.18	0.312
On Time	2	2.55	1.27	1.19	0.368
Current	2	2.39	1.20	1.09	0.395
Off Time	2	2.18	1.09	0.96	0.434

Table 9. Calculation error of regression equation (equation 5) and experimental result

Experimental number	Ra experimental result	Ra regression equation	Error %
1	3.22800	3.22804	10.880E-4
2	2.64767	2.64772	19.075E-4
3	4.98133	4.98140	12.982E-4
4	3.00967	3.00972	17.771E-4
5	5.53500	5.53506	11.467E-4
6	3.80967	3.80970	8.4010E-4
7	2.37800	2.37807	27.468E-4
8	2.95900	2.95904	12.842E-4
9	3.67300	3.67305	12.788E-4

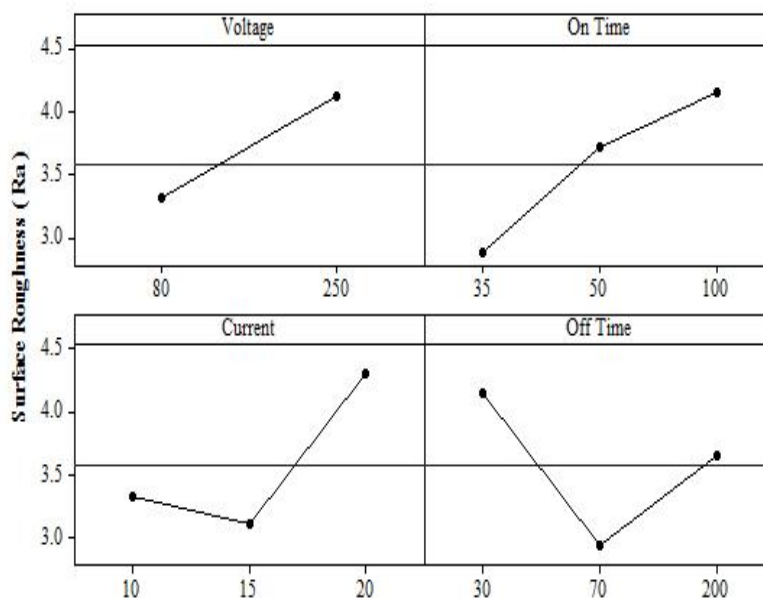


Figure 5. Effect of input parameters on surface roughness

5. CONCLUSION

In this study, a mathematical model based on practical experiments was introduced to evaluate material removal rate and surface roughness of NiTi60 shape memory alloy by means of copper electrode and de-ionized water. This mathematical model was achieved with Analysis of variance for 95% confidence level. Moreover, a meaningful relationship between EDM's input parameters including voltage, current pulse on time and pulse off time and output parameters including material removal rate and surface roughness was available by use of this model. The model showed that some of these parameters have less effect on material removal rate. Increase in current intensity has the most significant effect on surface roughness. Generally, the effect of each EDM's input parameter on output parameters can be studied using two suggested model for material removal rate and surface roughness. Furthermore, it's possible to achieve the desired surface roughness and material removal rate in addition to reduction in the number of experiments by changing the parameters in the suggested mathematical model.

References

1. V. Kumar, N. Beri, A. Kumar, *Journal of Advanced Engineering Technology*. 1 (2010) 16.
2. D. Bhaduri, A. S. Kuar, S. Sarkar, S. K. Biswas, S. Mitra, *Journal of Materials and Manufacturing Processes*. 24 (2009) 1312.
3. S. Daneshmand, E. Farahmand Kahrizi, E. Abedi, M. Mir Abdolhosseini, *International Journal of Electrochemical Science*. 8 (2013) 3095.
4. S. Saedodin, M. Torabi, H. Eskandar, *Journal of Advanced Design and Manufacturing Technology*. 3 (2010) 17.
5. H. El-Hofy, *Advanced Machining Processes Nontraditional and Hybrid Machining Processes*, McGraw-Hill. (2005) 120.

6. A. A. Lotfi, S. Daneshmand, *Journal of Advances in Materials Science and Engineering*. 2013 (2013) 6.
7. D.E. Hodgson, *Using Shape Memory Alloys, Shape memory Applications*, Inc., 1988
8. S. Daneshmand, E. Farahmand Kahrizi, A. A. Lotfi Neyestanak, M. Mortazavi Ghahi, *International Journal of Electrochemical Science*. 8 (2013) 7484.
9. H. Wu. Ming, and L. McD. Schetky, *Proceedings of the Conference on Shape Memory and Superelastic Technologies*, Pacific Grove, California, P.171-182 (2000).
10. J. Y. Kao, C. C. Tsao, S. S. Wang, C. Y. Hsu, *Journal of Advanced Manufacturing Technology*. 47 (2010) 395.
11. G. Indurkha, K.P. Rajurkar, *Proceedings of Artificial Neural Networks in Engineering Conference*, St. Louis, Missouri, U.S.A., 15-18 November. (1992) 845.
12. K. Niranjana Prasad, B. Ramamoorthy, *Journal of Materials Processing Technology*. 112 (2001) 43.
13. A. Z. Tomkiewicz, *Journal of Materials Processing Technology*. 109 (2001) 300.
14. X. Q. Li, Y. S. Wong and A. Y. C. Nee, *Journal of Manufacturing Science Engineering*. 120 (1998) 433.
15. Y.S. Tarng, T.C. Li, M.C. Chen, *Journal of Machine Tools and Manufacture*. 34 (1994) 949.
16. U. Fischer, M. Heinzle, F. Näher, H. Paetzold, R. Kilgus, R. Gomeringer, Oesterle, A.S. Stephan, *Tabellenbuch Metall*. Verlag Europa-Lehrmittel, Nourney, VollmerGmbH and Co. KG. (2008).
17. <http://www.Matweb.com>.
18. A. A. Lotfi, S. Daneshmand, S. Adib Nazari, *Journal of Advanced Design and Manufacturing Technology*. 2 (2009) 51.

© 2014 The Authors. Published by ESG (www.electrochemsci.org). This article is an open access article distributed under the terms and conditions of the Creative Commons Attribution license (<http://creativecommons.org/licenses/by/4.0/>).